UKACC International Conference on Control 2012
Cardiff, UK, 3-5 September 2012

# Model of a Fusion Cryopumping System for Condition Monitoring

Nick Wright
School of Electrical, Electronic and Systems Engineering
Loughborough University
Loughborough, Leics LE11 3TU
Email: n.wright@lboro.ac.uk

Roger Dixon
School of Electrical, Electronic and Systems Engineering
Loughborough University
Loughborough, Leics LE11 3TU
Email: r.dixon@lboro.ac.uk

Roel Verhoeven
Culham Centre for Fusion Energy
Culham Science Centre
Oxfordshire OX14 3DB
Email: roel.verhoeven@ccfe.ac.uk

***Abstract*—Cryopumping systems provide an essential function in most magnetic confinement nuclear fusion experiments. The maintenance of an ultra-high vacuum in a magnetic confinement vessel is required for experiments to be conducted, without exception, and cryopumping systems are widely used to achieve this. As such, the availability of this type of nuclear fusion experiment depends in part upon the availability of its vacuum system. In order to reduce experimental time lost to unplanned maintenance, investigation and avoidable failures, a condition monitoring scheme targeted on a cryopumping vacuum system is proposed. A model of the cryopumping system deployed on the Joint European Torus is presented. The model is supported by a first principles derivation and is validated using historical data. Its application to a condition monitoring scheme is discussed. This paper contributes to the wider nuclear fusion development programme by addressing a key maintenance and reliability issue, which is an important step on the road to commercial fusion energy.**

***Index Terms*—Condition Monitoring, Cryopumping, Dynamic Modelling, Two Phase Systems**

## I. Introduction

All nuclear fusion experiments using magnetic confinement techniques rely on the maintenance of an ultra-high vacuum inside the reaction vessel. This includes all the other vessels with which it shares an atmosphere. Any event that causes a disruption or loss of vacuum will result in the experiment being stopped while the vacuum is regenerated and the cause of the event mitigated. At the leading nuclear fusion experiment, the Joint European Torus (JET), and indeed at most others, loss of vacuum events and disruptions to the vacuum pumping system are identified, diagnosed and isolated manually. This process can be lengthy, requiring many man hours of labour. Time expended on maintenance is a significant burden, and as such there is a strong motivation for its reduction. Condition monitoring techniques have been used successfully in many applications, and it is proposed that such a condition monitoring scheme would be a very useful tool for the engineering team at JET. Historically, most disruptive and loss of vacuum events have occurred in the neutral beam heating systems, therefore a condition monitoring scheme focused on this area would be useful. In this paper we discuss a model of the cryopumping system deployed in the neutral beam heating devices at JET and how it can be used in the development of a condition monitoring scheme.

The neutral injection box (NIB) cryopump can be considered to be a two phase system. Two excellent examples of modelling two phase systems can be found in T Phillip's book on modelling and simulation[1] and in KJ Astrom's paper on drum boiler dynamics[2]. The novel model presented here is inspired by these examples. G Duesing's 1987 paper[3] is often referred to in discussions of neutral beam injection systems, and more recently, Ciric[4] and Ciric et al[5] wrote about recent developments in JET's NIB cryopumping scheme. These sources, in addition to design documentation available from CCFE, provide detailed information on the system discussed here. For information on cryogenic and vacuum systems in general, R Barron's book[6], WM Rohsenow's comprehensive book[7] and DJ Hucknall's book[8] are all excellent sources. A two phase model of a cryopumping system, however, has not yet been presented in literature. Using sources together has allowed us to develop a novel analytical model of the JET NIB cryopumping system which can serve both as tool for the design of a condition monitoring scheme and simulating faults.

This paper is split into four sections. The second section describes the physical system with which we are concerned. A justification of the selection of the target subsystem is provided, and its important features are discussed. The third section goes through the analytical model of the NIB cryopumping system and the fourth section presents the a result of a simulation of the model compared to historical data. The final section summarises the key information presented in this paper and notes its future application to condition monitoring.

## II. The Physical Cryopump

Cryopumping reduces the pressure inside a vacuum vessel by condensing gasses onto very cold surfaces. There are several ways to achieve this; RA Haefer describes some in his 1989 book[9]. The NIB cryopumping system at JET works by cooling a series of extruded aluminium surfaces inset with capillaries with cryogenic fluid. Each NIB has ten cryopump elements on each side of the vessel. Fig. 1 is a plan view illustration of a single cryopump element.

978-1-4673-1558-6/12/$31.00 ©2012 IEEE

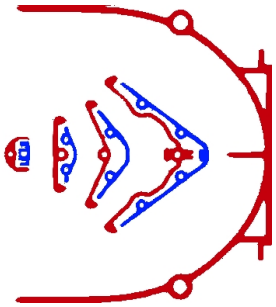

Fig. 1. A single cryopump element

Each cryopump element contains two types of surface: nitrogen surfaces and helium surfaces. The nitrogen surfaces are cooled to around 77K using liquid nitrogen. Similarly, the helium surfaces are cooled to around 4.2K, using liquid helium. In Fig. 1, the nitrogen surfaces have been drawn in red, the helium surfaces in blue. The purpose of the nitrogen surfaces is to shield the helium surfaces from thermal radiation and to pre-cool gas particles. The helium panels condense the majority of the gas. The capillaries embedded in the helium panels are filled from the bottom, and on the top they are tied-off onto a horizontal manifold and phase separator assembly.

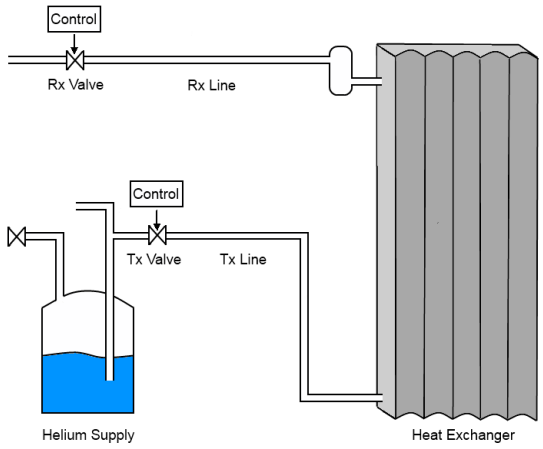


Fig. 2. Illustration of the NIB helium loop

Fig. 2 is a schematic of the NIB helium loop. The heat exchanger represents the two cryopumping walls. Also shown are the fluid/gas transmission and return line (labelled Tx and Rx lines), the transmission and return valves (labelled Tx and Rx valves), and the helium supply tank. The system boundaries are the helium source from which the helium tank is filled, and the helium return valve box, where gaseous helium evolved from the heat exchanger is diverted to either the helium liquefiers or helium collection balloons.

The helium transmission and return lines are part of the same assembly. Liquid helium, liquid nitrogen, gaseous helium and gaseous nitrogen are all carried in a single transmission line, comprised of several concentric cylinders. Together with a vacuum jacket, the cylinders are arranged in such a way as to minimise thermal losses. Between the helium supply tank and the helium return valve box are two valves: the helium supply and return valves. Each valve is designed to minimise thermal losses. They act as control valves, each with a standard feedback PI scheme. The control variable for the supply valve is the level of fluid in the phase separator and the control variable for the return valve is the (absolute) pressure in the helium return line. The helium supply tank is periodically filled, according to the fluid level. Helium inside the tank is distributed to four places: the two NIBs, a cooling system in the supply valve box and to a helium liquefier (to deal with tank losses). Helium inside the tank is maintained at a constant pressure.

A list of measured process variables on the helium loop is presented in Table I. While each of these process variables is available in real time, a recording is only made once an unscaled variable deviates two percent from its previously recorded value.

| Process variable | Unit |
|---|---|
| Phase separator level | % |
| Supply & return valve position | % |
| Supply & return line pressure | BarA and BarG |
| Capillary delta pressure | mBar |
| Helium supply temperature | K |
| Helium return temperature | K |
| Helium tank fill level | % |
| Helium tank fill volume | l |

TABLE I
LIST OF MEASURED PROCESS VARIABLES

The specific (latent) heat capacity of liquid helium is low and the helium panels are sensitive to heat load. This, in addition to the high level of instrumentation on the helium panel support system (the helium loop), means that information about the state of the NIB vacuum can be deduced from examination of the state of the helium loop. Furthermore, historically, the helium loop has experienced more maintenance issues than the nitrogen loop, and several (potential) loss of vacuum events relating to faults in the helium line were identified in a simplified FMEA process. For these reasons, it was decided that the initial focus for the condition monitoring scheme should be on the helium loop. It should also be noted that the cryopump has several operational modes. The mode focused on here is the "full cooldown" mode, which the pumping system is set to during regular operation (i.e. Most of the time outside of scheduled maintenance periods).

## III. The Model Cryopump

The mathematical model of the helium loop in the cryopumping system is split into nine component models, roughly corresponding with the components depicted in Fig. 2. In order to provide structure to the model, the component models have been categorised as either storage or resistive components, allowing a common interface between them and simplifying their analysis. Specifically, the storage components have a pressure associated with them; the resistive components, a flow

rate. Fig. 3 is an illustration of this structure. A description of each of these blocks is presented below, starting with the supporting blocks and moving on to the main block, the heat exchanger.

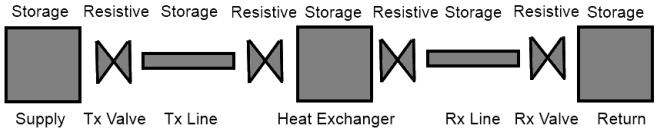


Fig. 3. Model structure

### A. Supporting Blocks

Starting with the supply and return (boundary) blocks, the following assumptions were made:

(a) The helium tank is always refilled at the appropriate times
(b) When the tank is being refilled, it is refilled at a constant, uninterrupted rate
(c) The pressure on the return side of the return valve is controlled and constant
(d) The helium supply pressure and temperature is constant
(e) The helium consumption in both NIBs is similar and converges with time
(f) Helium tank losses (and hence the amount of material sent to the liquefier) are negligible

Given these assumptions, the following equation described the the helium tank fluid volume:

$$\frac{dV_{ht}}{dt} = K_{kl} q_{tf} - K_{kl} \left( q_{sc} + q_{ts} + 2q_{tl} \right) \tag{1}$$

where $V_{ht}$ is the fluid volume in the helium tank, $q_{tf}$ is the helium tank fill rate, $q_{sc}$ is the flow rate to the valve box subcooler, $q_{ts}$ is the flow rate of tank losses, and $q_{tl}$ is the flow rate to the (single) NIB transmission line.

The transmission and return control valves are treated independently, because the former controls the flow of a (relatively, compared to helium gas) incompressible fluid and the latter, compressible helium gas. They are both resistive components. The flow rate through the transmission valve is described by:

$$q_{fl} = Y_{tx} C_v \sqrt{\frac{\Delta p}{v_i}} \tag{2}$$

where $C_v$ is the valve conductance, $\Delta p$ is the differential pressure across the valve, $Y_{tx}$ is the proportion the valve is open, normalised between zero and unity, and $v_i$ is the specific volume of the fluid at the valve inlet.

The return valve is described using an equation for valves transmitting compressible gasses referred to by Baumann[10]:

$$q_{rl} = Y_{rx} C_v 3.22 \sqrt{\Delta p \left( p_1 + p_2 \right) G_g} \tag{3}$$

where, with care to use US units for all the terms and converting afterwards, owing to the empirical scaling factor, $q_{rl}$ is the return valve flow rate and $G_g$ is the specific gravity of the gas.

The transmission lines are storage components. They are assumed to be of fixed volume, regardless of pressure (historically, pressure deviates no more than 10% from its mean). For the return line, making ideal gas assumptions, the pressure is given by the well known equation:

$$p_{rl} = \frac{nRT_{rl}}{V_{rl}} \tag{4}$$

where the subscript $rl$ referes to the return line.
The supply line pressure is given by:

$$p_{tl} = \int \left( q_{tl} - q_f \right) \frac{B}{V_{tl}} + p_{hyd} \tag{5}$$

where the subscript $tl$ refers to the transmission line, $B$ is the bulk modulus of the helium fluid. $p_{hyd}$ represents hydrostatic pressure, which is given by:

$$p_{hyd} = h \rho g \tag{6}$$

where $h$ the height of the fluid in the heat exchanger capillaries and phase separator and $g$ is acceleration due to gravity.

It should be noted that, whilst liquid helium is more compressible than many other fluids (with commonly assumed bulk modulus of 268 Bar[11], although this varies with temperature), a high pressure change (in the context of this system) is required to significantly reduce its volume. Under normal conditions, helium is typically compressed no more than 1%. Hemce it can be assumed that the pressure in the transmission line is equivalent to the pressure inside the heat exchanger plus the hydrostatic pressure component.

In Fig. 3, two resistive blocks are set either side of the storage component of the heat exchanger. These blocks are treated the same as the valve blocks described in (2) and (3), with $Y$ set to unity and a conductance representative of the constriction between the transmission line and heat exchanger.

### B. Heat Exchanger

Finally, the heat exchanger block is considered. This block requires a more in depth analysis for its behaviour to be described in sufficient detail. There are several different ways to model this section of the system; the technique used here is to take a mass and energy balance across this section's boundaries.

Fig. 4 is an illustration of the capillaries and phase separator as modelled. The top section of the diagram represents the phase separator, with the horizontal return manifold attached, the bottom section represents the capillaries. The distribution of the cryogenic fluid between the capillaries is not relevant and so the capillaries are treated as a lumped element. $Q$, $q_f$ and $q_s$ are the main inputs and outputs to the system. They are, respectively, heat load, fluid flow rate into the capillaries and vapour flow rate. The fluid level in the phase separator is labelled $l$ and the system pressure and temperature are represented by $T$ and $P$.

The following assumptions have been made: The capillaries (risers) are treated as a lumped construction, this entire

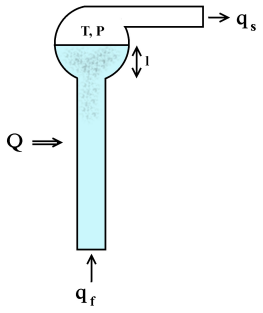


Fig. 4. Phase separator and capillary layout

section is in thermal equilibrium, and the phase separator contains a saturated vapour-fluid mixture. These assumptions are supported by historical process data and represent that real working of the system well. In the coming analysis, the terms $Q$, $q$, $h$, $V$ and $\rho$ represent, heat, flow rate, specific enthalpy and volume respectively. The subscripts '$s$', '$f$', '$w$' and '$t$' refer to vapour, feed, fluid and total respectively. SI units are used unless otherwise stated. This portion of the model is derived as follows.

*1) Global Mass and Energy Balance:* To begin with, the global mass balance of the system is described by:

$$\frac{d}{dt}\left[\rho_s V_{st} + \rho_w V_{wt}\right] = q_f - q_s \tag{7}$$

And the energy balance of the system is:

$$\frac{d}{dt}\left[\rho_s V_{st} u_s + \rho_w V_{wt} u_w + m_t C_p t_m\right] = Q + q_f h_f - q_s h_s \tag{8}$$

Now, the well known relationship between specific enthalpy and specific energy

$$u = h - \frac{p}{\rho} = h - pV \tag{9}$$

is substituted into equation 8 to give a global energy balance:

$$\begin{aligned}&\frac{d}{dt}\left[\rho_s V_{st} h_s + \rho_w V_{wt} h_w + m_t C_p t_m - pV_t\right]\\ &= Q + q_f h_f - q_s h_s\end{aligned} \tag{10}$$

*2) Local Mass and Energy Balances:* To describe the distribution of vapour of fluid in the phase separator we start with the relationship between their volumes:

$$V_t = V_{st} + V_{wt} \tag{11}$$

And condensation enthalpy is represented by $h_c$.

With this property defined, the next step is to examine the mass and energy balance in the capillaries. In the analysis of other two-phase boiler systems (for example, power plant boilers), often the term "steam quality" is used to describe the proportion of vapour to fluid at a given location.

The mass fraction of vapour in the capillaries (steam quality) here is described by:

$$\alpha_m = \frac{QA}{qh_c V} z \tag{12}$$

If $\xi$ is the normalised length coordinate along the riser ($0 \leq \xi \leq 1$), then:

$$\alpha_m = \alpha_r \xi \tag{13}$$

Steam slip is a measure of the relative average velocities of liquid and gas phases in two phase flow. In this model it is assumed that steam slip is negligible, as its inclusion significantly increases the complexity of the analysis while not contributing significantly to the output of the model. For similar reasons, it is assumed the the boiling and vapour nucleation process begins at the bottom of the capillary tubes.

The average steam volume ratio in the capillaries is given by:

$$\begin{aligned}\overline{\alpha}_v = \frac{\rho_w}{\rho_w - \rho_s}\Big[1 - \frac{\rho_s}{(\rho_w - \rho_s)\,\alpha_r}\\ \ln\left(1 + \frac{\rho_w - \rho_s}{\rho_s}\alpha_r\right)\Big]\end{aligned} \tag{14}$$

Using this relation, the capillary mass balance is given by:

$$\frac{d}{dt}\left[\rho_s \overline{\alpha}_v V_r + \rho_w\left(1 - \overline{\alpha}_v\right) V_r\right] = q_f - q_r \tag{15}$$

Then from this and 9, the capillary energy balance is:

$$\begin{aligned}&\frac{d}{dt}\left[\rho_s h_s \overline{\alpha}_v V_r + \rho_w h_w\left(1 - \overline{\alpha}_v\right) V_r - pV_r + m_r C_p t_s\right]\\ &= Q + q_f h_f - \left(\alpha_r h_c + h_w\right) q_r\end{aligned} \tag{16}$$

With the mass and energy balance in the capillaries accounted for, the dynamics of the phase separator and the distribution of vapour within it remain to be analysed.

The volume of vapour in the phase separator under the fluid level is given by:

$$\frac{d}{dt}\left[\rho_s V_{sd}\right] = \alpha_r q_r - q_{sd} - q_{cd} \tag{17}$$

where the condensation flow rate in the phase separator is given by:

$$\begin{aligned}q_{cd} = \frac{1}{h_c}\Big[\rho_s V_{sd}\frac{dh_s}{dt} + \rho_w V_{wd}\frac{dh_w}{dt}\\ - \left(V_{sd} + Vwd\right)\frac{dp}{dt} + m_d C_p \frac{dt_s}{dt}\Big]\end{aligned} \tag{18}$$

The flow rate of vapour through the surface is calculated from the velocity and volume of vapour bubbles leaving the risers:

$$q_{sd} = \frac{\rho_s V_{sd}\left[1.53\frac{\sigma g(\rho_w - \rho_s)}{\rho_w^2}\right]^{\frac{1}{4}}}{l} \tag{19}$$

The volume of fluid inside the phase separator is obtained by subtracting the amount of fluid in the capillaries from the total amount of fluid in the system:

$$V_{wd} = V_{wt} - (1 - \overline{\alpha}_v) V_r \tag{20}$$

This allows the fluid level in the phase separator to be calculated:

$$\text{level}(\%) = 50 + \left[\arcsin\left(2\frac{V_{wd} + V_{sd}}{V_t}\right) - 1\right]\frac{50}{90} \tag{21}$$

where the trigonometric function is in degrees and the fill level of the phase separator is between 0 and 100 %.

*3) Dynamics of the Capillaries and Phase Separator:* In order to describe the mass flow rates of vapour and fluid through the capillaries and phase separator, first the capillary mass balance described in 15 is multiplied by $-(h_w + \alpha_r h_c)$:

$$\begin{aligned}&\frac{d}{dt}\left[\rho_s\overline{\alpha}_v V_r + \rho_w(1-\overline{\alpha}_v)V_r\right]\left[-(h_w + \alpha_r h_c)\right]\\ &= \left[q_f - q_r\right]\left[-(h_w + \alpha_r h_c)\right]\end{aligned} \tag{22}$$

Then this is added to the capillary energy balance, given in 16:

$$\begin{aligned}&\frac{d}{dt}\left(\rho_s\overline{\alpha}_v h_s V_r\right) - (h_w + \alpha_r h_c)\frac{d}{dt}\left(\rho_s\overline{\alpha}_v V_r\right)\\ &+ \frac{d}{dt}\left(\rho_w h_w (1-\overline{\alpha}_v)V_r\right)\\ &- (h_w + \alpha_r h_c)\frac{d}{dt}\left(\rho_w(1-\overline{\alpha}_v)V_r\right) - V_r\frac{dp}{dt} + m_r C_p\frac{dt_s}{dt}\\ &= Q + q_f h_f - (\alpha_r h_c + h_w)q_r - (q_f - q_r)(h_w + \alpha_r h_c)\\ &= Q + q_f h_f - q_f h_w - q_f\alpha_r h_c\\ &= Q + q_f(h_f - h_w - \alpha_r h_c)\end{aligned} \tag{23}$$

This simplifies to:

$$\begin{aligned}&h_c(1-\alpha_r)\frac{d}{dt}\left(\rho_s\overline{\alpha}_v V_r\right) + \rho_w(1-\overline{\alpha}_v)V_r\frac{dh_w}{dt}\\ &- \alpha_r h_c\frac{d}{dt}\left(\rho_w(1-\overline{\alpha}_v)V_r\right) + \rho_s\overline{\alpha}_v V_r\frac{dh_s}{dt}\\ &- V_r\frac{dp}{dt} + m_r C_p\frac{dt_s}{dt} = Q + q_f(h_f - h_w - \alpha_r h_c)\end{aligned} \tag{24}$$

To derive an equation for the capillary flow rate, $q_r$, 15 is rearranged into terms of $p$ and $\alpha_r$:

$$\begin{aligned}q_r &= q_f - \frac{d}{dt}\left[\rho_s\overline{\alpha}_v V_r + \rho_w(1-\overline{\alpha}_v)V_r\right]\\ &= q_f - V_r\frac{d}{dt}\left((1-\overline{\alpha}_v)\rho_w + \overline{\alpha}_v\rho_s\right)\\ &= q_f - V_r\frac{d}{dp}\left[(1-\overline{\alpha}_v)\rho_w + \overline{\alpha}_v\rho_s\right]\frac{dp}{dt}\\ &+ V_r(\rho_s - \rho_w)\frac{d\overline{\alpha}_v}{d\alpha_r}\frac{d\alpha_r}{dt}\end{aligned} \tag{25}$$

The final step is to derive an expression for the dynamics of the vapour in the phase separator. Substituting the mass equations for $q_{cd}$, $q_{sd}$ and $q_r$ (equations 18, 19 and 25) into the vapour balance equation (17) gives:

$$\begin{aligned}&\rho_s\frac{dV_{sd}}{dt} + V_{sd}\frac{d\rho_s}{dt}\\ &= \alpha_r\Big(q_f - V_r\frac{d}{dp}\left[(1-\overline{\alpha}_v)\rho_w + \overline{\alpha}_v\rho_s\right]\frac{dp}{dt}\\ &+ V_r(\rho_w - \rho_s)\frac{d\overline{\alpha}_v}{d\alpha_r}\frac{d\alpha_r}{dt}\Big)\\ &- \frac{\rho_s V_{sd}\left[1.53\frac{\sigma g(\rho_w - \rho_s)}{\rho_w^2}\right]^{\frac{1}{4}}}{l}\\ &- \frac{1}{h_c}\Big(\rho_s V_{sd}\frac{dh_s}{dt} + \rho_w V_{wd}\frac{dh_w}{dt}\\ &- \left[V_{sd} + V_{wd}\right]\frac{dp}{dt} + m_d C_p\frac{dt_s}{dt}\Big)\end{aligned} \tag{26}$$

Which can be rearranged to:

$$\begin{aligned}&\rho_s\frac{dV_{sd}}{dt} + V_{sd}\frac{d\rho_s}{dt}\\ &- \alpha_r\Big(-V_r\frac{d}{dp}\left[(1-\overline{\alpha}_v)\rho_w + \overline{\alpha}_v\rho_s\right]\frac{dp}{dt}\\ &+ V_r(\rho_w - \rho_s)\frac{d\overline{\alpha}_v}{d\alpha_r}\frac{d\alpha_r}{dt}\Big)\\ &+ \frac{1}{h_c}\Big(\rho_s V_{sd}\frac{dh_s}{dt} + \rho_w V_{wd}\frac{dh_w}{dt}\\ &- \left[V_{sd} + V_{wd}\right]\frac{dp}{dt} + m_d C_p\frac{dt_s}{dt}\Big)\\ &= \alpha_r q_f + \left(\frac{\rho_s V_{sd}\left[1.53\frac{\sigma g(\rho_w - \rho_s)}{\rho_w^2}\right]^{\frac{1}{4}}}{l}\right)\end{aligned} \tag{27}$$

*4) Non-linear State Variables:* Using four state variables, a full set of set of state equations that describe this section of the model can be developed. The four state variables are pressure, steam quality at the capillary-phase separator junction, total volume of fluid and volume of vapour under the fluid level ($p$, $\alpha_r$, $V_{wt}$ and $V_{sd}$). The state equations describing the heat exchanger take the following form, where the $e$ terms are found by collecting terms in the equations highlighted below. Saturated steam tables are used to evaluate the thermodynamic terms.

From 7, 10 and 11:

$$e_{11}\frac{dV_{wt}}{dt} + e_{12}\frac{dp}{dt} = q_f - q_s \tag{28}$$

$$e_{21}\frac{dV_{wt}}{dt} + e_{12}\frac{dp}{dt} = Q + q_f h_f - q_s h_s \tag{29}$$

and 24 and 27:

$$e_{32}\frac{dp}{dt} + e_{33}\frac{d\alpha_r}{dt} = Q + q_f(h_f - h_w - \alpha_r h_c) \tag{30}$$

$$e_{42}\frac{dp}{dt} + e_{43}\frac{d\alpha_r}{dt} + e_{44}\frac{dV_{sd}}{dt} = \alpha_r q_f + \left( \frac{\rho_s V_{sd}\left[1.53\frac{\sigma g(\rho_w - \rho_s)}{\rho_w^2}\right]^{\frac{1}{4}}}{l} \right) \quad (31)$$

## IV. Validation

This model is implimented in Matlab/Simulink using a combination of standard blocks and s-functions, and the output of the simulation was compared to data recorded at JET on the NIB4 cryopumping system. The two simulation results presented below are compared to data from the morning of February 21, 2012. The inputs to the simulation were historically measured supply valve position and a heat load corresponding to the experiment shots run that morning. The physical parameters (sizes, masses, conductances and boundary pressures) of the model were set according to design data provided by CCFE.

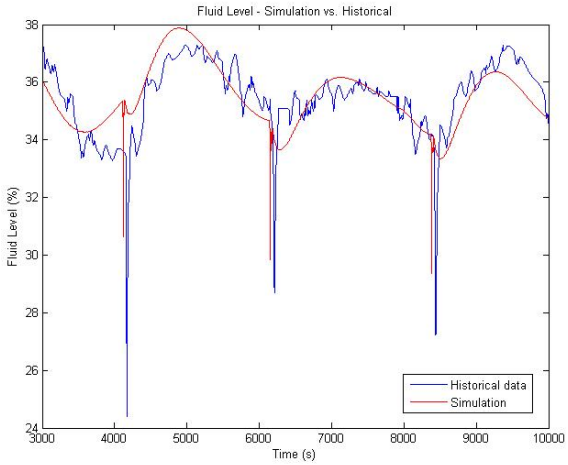


Fig. 5. Phase separator fluid level

Fig. 5 and 6 show the most interesting features of the simulation. The simulation tracks the historical process data to within 1% of the total variable range (1 to 100%) in both cases for most of the time shown. This suggests that the model describes the system well enough to simulate and predict the important system behaviors.

Each of the three salient points corresponds to the occurrence of a shot. A typical shot results in an additional heat load of around 20W on the helium panels for one or two seconds, followed by a lower heat load of around 3W for a further thirty seconds. Both the fluid level and return valve position appear to be sensitive to small heat loads on the cryopumping system, compared to the base load heat from the panel supports and thermal radiation of nearby components of close to 104W. As such, these are potentially useful variables to consider when designing a scheme to detect faults resulting in excessive heat load, such as loss of vacuum events.

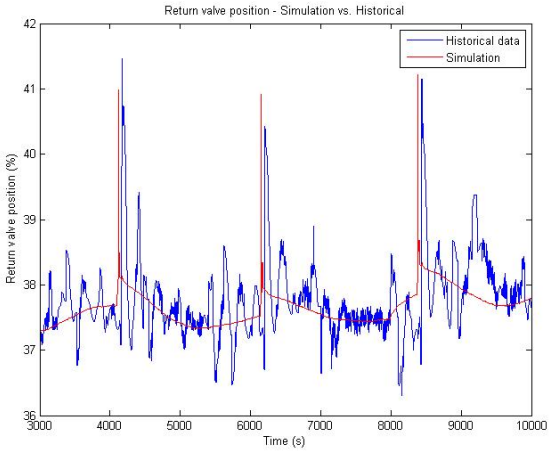


Fig. 6. Return valve position

## V. Conclusion

A novel analytical model of a large two phase cryopumping system has been derived from first principles and validated using historical data. Dividing the cryopump into resistive and storage components is a suitable technique for modelling such systems. From a Matlab/Simulink simulation it was found that phase separator fluid level and return valve position are highly sensitive to extra heat load on the cryopumping system. This suggests that the model could be used in the design of a condition monitoring scheme to detect loss of vacuum events.

Future work will see this model used to design a condition monitoring scheme, making use of the parity equations approach. This model could also be used as a basis for developing simulations of faults and could also be used as part of a model based control design process.

## Acknowledgment

This research is being conducted on behalf of CCFE and is funded by EPSRC, as a CASE studentship.

## References

[1] T. Philip, *Simulation of industrial processes for control engineers*. Butterworth-Heinemann, 1999.
[2] K. Aström and R. Bell, "Drum-boiler dynamics," *Automatica*, vol. 36, no. 3, pp. 363–378, Mar. 2000.
[3] G. Duesing, "The vacuum systems of the nuclear fusion facility JET," *Vacuum*, vol. 37, no. 3-4, pp. 309–315, 1987.
[4] D. Ciric, "Neutral Beam Heating Overview," Culham Centre for Fusion Energy, Culham, Tech. Rep., 2008.
[5] D. Ciric *et al.*, "Overview of the JET neutral beam enhancement project," *Fusion Engineering and Design*, vol. 82, no. 5-14, pp. 610–618, Oct. 2007.
[6] R. F. Barron, *Cryogenic heat transfer*. Taylor and Francis, 1999.
[7] W. Rohsenow, J. Hartnett, and E. Ganic, *Handbook of heat transfer fundamentals*, second edi ed. McGraw-Hill, 1985.
[8] D. Hucknall and A. Morris, *Vacuum technology: calculations in chemistry*. Royal Society of Chemistry, 2003.
[9] R. A. Haefer, *Cryopumping: theory and practice*. Clarendon Press, 1989.
[10] H. D. Baumann, *Control Valve Primer: A User's Guide*. ISA, 2009.
[11] E. R. Grilly, "Pressure-volume-temperature relations in liquid and solid4He," *Journal of Low Temperature Physics*, vol. 11, no. 1-2, pp. 33–52, Apr. 1973.